Reduction of granular drag inspired by self-burrowing rotary seeds

Wonjong Jung, Sung Mok Choi, Wonjung Kim, and Ho-Young Kim

Citation: Physics of Fluids **29**, 041702 (2017); doi: 10.1063/1.4979998
View online: http://dx.doi.org/10.1063/1.4979998
View Table of Contents: http://aip.scitation.org/toc/phf/29/4
Published by the American Institute of Physics

Reduction of granular drag inspired by self-burrowing rotary seeds

Wonjong Jung,[1] Sung Mok Choi,[1] Wonjung Kim,[2,a)] and Ho-Young Kim[1,3,b)]
[1]*Department of Mechanical and Aerospace Engineering, Seoul National University, Seoul 08826, South Korea*
[2]*Department of Mechanical Engineering, Sogang University, Seoul 04107, South Korea*
[3]*Urban Data Science Lab, SNU BDI, Seoul 06324, South Korea*

(Received 13 February 2017; accepted 29 March 2017; published online 18 April 2017)

We present quantitative measurements and mathematical analysis of the granular drag reduction by rotation, as motivated by the digging of *Erodium* and *Pelargonium* seeds. The seeds create a motion to dig into soil before germination using their moisture-responsive awns, which are originally helical shaped but reversibly deform to a linear configuration in a humid environment. We show that the rotation greatly lowers the resistance of soil against penetration because grain rearrangements near the intruder change the force chain network. We find a general correlation for the drag reduction by relative slip, leading to a mathematical model for the granular drag of a rotating intruder. In addition to shedding light on the mechanics of a rotating body in granular media, this work can guide us to design robots working in granular media with enhanced maneuverability. *Published by AIP Publishing.* [http://dx.doi.org/10.1063/1.4979998]

Ingenious mobility strategies have been evolved in animals[1–5] and plant roots[6,7] in a granular environment such as soil, where mobility is significantly reduced by intergranular resistance. Some *Erodium* and *Pelargonium* species, flowering plants belonging to a genus of the family Geraniaceae, produce seeds with an appendage that is used for the seed dispersal and burial.[8–12] Fig. 1 (Multimedia view) shows the seed awns of three *Pelargonium* species. Each awn is composed of materials with different hygroscopic expansiveness and thus responds to a change in humidity.[11,12] In a humid environment at night time or after a rain fall, a helically coiled awn deforms to a linear configuration, and the deformation can create thrust against the soil when one end of the awn is anchored.[8] Owing to the helical shape of the awn, the hygroscopic expansion entails a rotary motion during the extension. This locomotory scheme reminds us of a conventional drilling machine or an auger with a rotational intruder, so it is highly probable that the seeds spin themselves to facilitate the digging into soil.

Granular drag on a body in quasi-static motion is mainly associated with the forces for breaking intergranular contacts in a jammed granular medium.[13–15] The jamming and relaxation of grains cause stick-slip,[14] pressure-screening,[20] and visco-elastic behaviors.[21] When a rod rotates horizontally, it disturbs the arrangement of the jammed grains, so that the rotational torque dramatically decreases after half a turn at a given depth.[22] Although a few mathematical models for granular drags are available under limited conditions,[22–24] understanding of the drag force for a vertically penetrating rotary intruder remains incomplete due to complicated intergranular mechanics.

Motivated by the self-burrowing rotary seeds, we here elucidate the reduction of granular drag by rotation for a vertically penetrating intruder. We found that the vertical drag against a rotating intruder decreases with its rotational speed. Noting that the relative motions of the grains in contact with the intruder induce the collapse of the force chains in the granular bulk, we developed a model for the drag reduction by rotation in terms of the slip velocity of the grains, which successfully explains the drag reduction of the rotating intruders.

We start with quantifying the drag reduction experienced by the biological examples through their rotation. We measured the granular resistance of seeds of three *Pelargonium* species during their vertical penetration in a granular medium. Fig. 2(a) illustrates the experimental setup to measure the drag forces. The seeds were forced into soil with a constant speed $v = 0.2$ mm/s in the container, whose diameter is 95 mm and height is 50 mm, filled with glass beads of a diameter ranging from 250 to 500 μm, and the drag forces were measured by a load cell. As shown in Fig. 2(b), the drag force depends on the shape and size of the seed head but increases with the burial depth for all cases. To test the drag reduction by spinning, we rotated the container of the glass beads around the axis of the seed at a rate of 7 rpm (the maximum rotational speed observed for a wet awn) at a burial depth of 1.5 mm as thrusting the seed at $v = 0.2$ mm/s. The granular resistance significantly decreased for all seeds by up to 75% in Fig. 2(b), demonstrating that a self-burrowing seed can indeed reduce the granular drag with its rotational motion.

We develop a mathematical model to understand this marked reduction of granular drag. The importance of the dynamic friction relative to static friction depends on the inertial number $I = \dot{\gamma} d/(P/\rho)^{1/2}$, where $\dot{\gamma}$ is the shear rate, d is the grain diameter, P is the hydrostatic pressure, and ρ is the density of grain.[25–27] In our experiment, the maximum rotational speed is 10 rpm, indicating the angular velocity $\omega \sim 1$ rad/s, so that the tangential velocity of the rotating intruder $v_r \sim \omega r \sim 1$ mm/s where the radius of rotation r is on the order the seed thickness (1 mm), and the shear rate

a)Electronic address: wonjungkim@sogang.ac.kr
b)Electronic address: hyk@snu.ac.kr

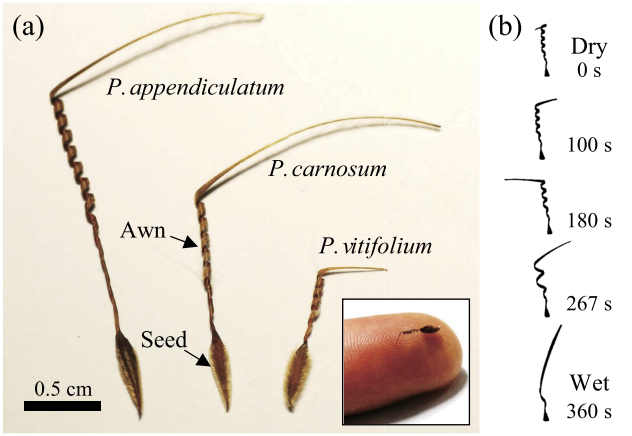

FIG. 1. Seeds of *Pelargonium* species. (a) Three *Pelargonium* species seeds with hygroscopically responsive awns: *P. appendiculatum* (left), *P. carnosum* (middle), and *P. vitifolium* (right). Inset image indicates the size of a seed of *P. vitifolium* in comparison with a human finger. (b) The helical awn of *P. carnosum* spontaneously uncoils to a linear configuration in a humid environment. (Multimedia view) [URL: http://dx.doi.org/10.1063/1.4979998.1] [URL: http://dx.doi.org/10.1063/1.4979998.2]

$\dot{\gamma} < (v^2 + v_r^2)^{1/2}/d \sim 3\ \mathrm{s}^{-1}$. In addition, $P = \rho g l \sim 0.25$ kPa, where g is the gravitational acceleration, $l = 10$ mm is the burial depth, and $\rho = 2.5$ g/cm^3. Hence, the inertial number $I < 3 \times 10^{-3}$, indicating a quasi-static flow regime,[25–27] in which the granular resistance depends exclusively on the static friction. Therefore, the normal force by static pressure on the intruder surface is mainly responsible for the drag.[28]

Consider a conical intruder with an apex at a distance l below the free surface, as shown in Fig. 2(a). We express the vertical force acting on the differential volume with a thickness of dz at the depth z from the free surface as $\mathrm{d}F(z) \sim \mu P \mathrm{d}A_s \sin\theta$, where μ is the internal friction coefficient, θ is the apex half angle of the conical intruder, and $\mathrm{d}A_s$ is the surface area of the intruder element. With $\mathrm{d}A_s = 2\pi(l - z)(\tan\theta/\cos\theta)\mathrm{d}z$ and $P = \rho g z$, integration of $\mathrm{d}F(z)$ with respect to z from 0 to l yields $F \sim (\pi/3)\mu\rho g l^3 \tan^2\theta$. If we define the effective resisting area $A_e = (\pi/3)l^2 \tan^2\theta$, the drag force can be simply expressed as $F \sim \mu P_t A_e$, where $P_t = \rho g l$ is the hydrostatic pressure at the intruder tip. Therefore, the granular drag increases with the apex half angle and burial depth. We experimentally examined the drag on the conical intruders with various apex half angles θ of 20°, 30°, and 45° to the burial depth of about three seed lengths. Fig. 2(c) presents the drag forces on the intruders, and the data points collapse onto a line predicted by the model, $F/\tan^2\theta \sim l^3$ (see inset in Fig. 2(c)).

We briefly discuss the advantage of the conical shapes of *Pelargonium* seeds for the self-burial behavior. In the quasi-static flow regime, the granular drag is given by $F \sim \mu\rho g l A_e$, where lA_e corresponds to the effective submerged volume of the intruder in granular media. Therefore, a small effective submerged volume of the intruder is advantageous for reducing the granular drag in self-burrowing. For instance, a seed with a conical shape with an effective submerged volume of $(\pi/3)l^3 \tan^2\theta$ can reduce the drag force by 1/3 compared with a seed with a cylindrical shape with a radius of $l\tan\theta$ for a given burial depth of l.

We measured the granular drag for the intruder with $\theta = 45°$ in a container rotating with a speed ranging from 0.2 to 10 rpm. The upper limit of the rotational speed was selected so as to remain in the quasi-static flow regime. In

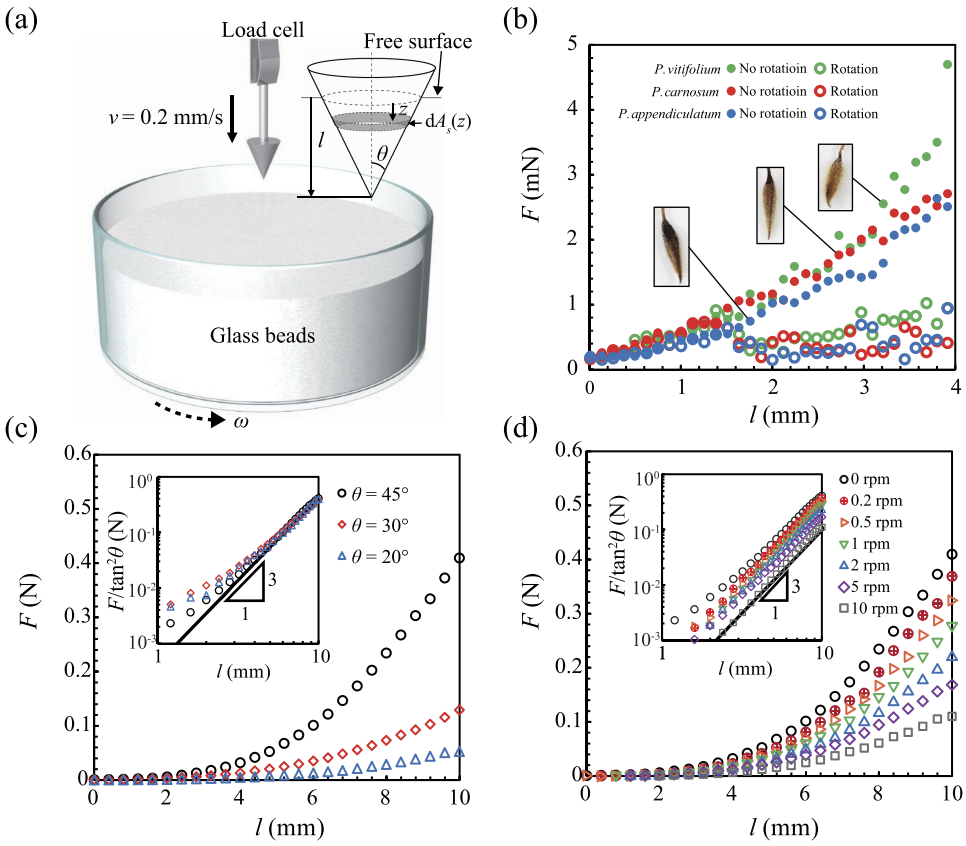

FIG. 2. Measurement of drag force. (a) Schematic illustration of an experimental setup to measure the drag force for the vertical penetration of the seed or intruder. (b) Dependence of the average drag force ($n = 5$, where n is the number of experiments) on the burial depth, l. Filled and empty symbols correspond to the drag force without rotation and with rotation, respectively. (c) Drag forces F for the conical intruders with the various apex half angles. Inset shows that $F/\tan^2\theta$ is proportional to l^3. (d) Granular drag for a rotating intruder with $\theta = 45°$. Inset shows that rotation does not change the cubic dependence. All measurement points for the conical intruders indicate average values ($n = 3$).

Fig. 2(d), the drag force is compared with that for an intruder without rotation. We see that the drag force decreases with the rotational speed, and the reduction reaches approximately 75% for the highest rotational speed of 10 rpm in our experiments. At this rotational speed, we measured the torque to rotate the intruder $\tau = 9 \times 10^{-5}$ Nm at a burial depth of 10 mm, so that the shear force by the granular medium is scaled as $F_{\text{shear}} \sim \tau / r_{\text{eff}} \sim 18 \times 10^{-3}$ N, where the radius of rotation r_{eff} = 5 mm was taken to be half the base radius of the submerged intruder. We calculate $F_{\text{shear}}/F \sim 0.045$, where the vertical drag force F is approximately 0.4 N (see Fig. 2(c)), and thus the shear force is insignificant compared with the vertical force. We also found that the rotation of the intruder reduces only the magnitude of the drag without a change in the cubic dependence on the burial depth l, implying that the normal static force is still responsible for the granular drag for the rotating intruder. This suggests that the intruder rotation reduces the effective resisting area A_e on which the granular hydrostatic pressure acts.

To aid the understanding of the drag reduction by rotation, we present the schematic of the grains beneath the bottom of a rotating intruder in Fig. 3. A penetrating intruder encounters force chains that resist its motion. Force chains are a network of intergranular contacts in the bulk medium, and granular hydrostatic pressure acts on the intruder surface along the force chains.[13–15] The rotation of intruder yields additional intergranular motions, which facilitate breaking of the force chains,[16–19] thereby reducing the vertical drag forces. The local surface speed induced by rotation increases with the radial distance from the intruder centerline, so the grains easily slip in the outer region. In contrast, the force chains are robust in the inner region where the surface speed is relatively low.

To quantify the drag reduction by slip motions between the intruder and grains, we experimentally examined the drag reduction ratio with respect to the slip velocity. As shown in Fig. 4(a), we measured the vertical drag force for the cylindrical intruder with a radius of 10 mm in a container filled with glass beads while the container translates in the direction orthogonal to that of penetration. It is observed that the drag decreases with the slip velocity, v_s. Furthermore, we see that the drag reduction ratio depends critically on the relative slip velocity $u = v_s/v$ in the quasi-static flow regime (see Fig. 4(a)).

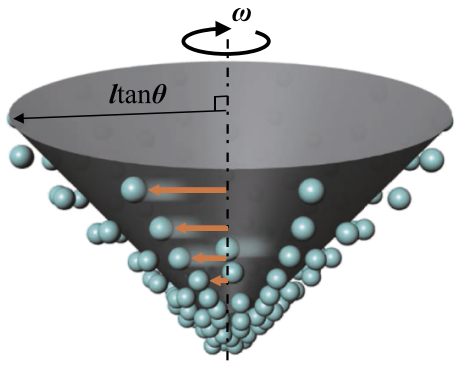

FIG. 3. Schematic illustration of the motion of grains underneath the rotating intruder. The rotational motion yields the intergranular motions which facilitate breaking the force chain network near the intruder.

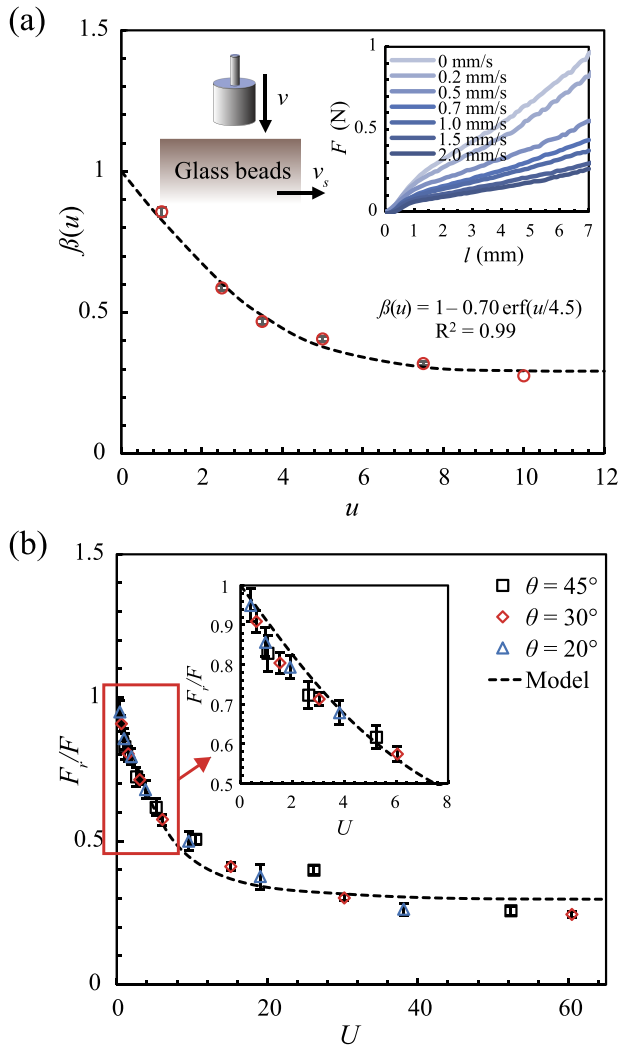

FIG. 4. Drag reduction by rotational motions. (a) Relative drag force for the cylindrical intruder with a slip to that with $u = 0$. The horizontal velocity v_s of glass beads ranges from 0.2 to 2.0 mm/s while the penetrating velocity v is 0.2 mm/s. The dashed line indicates our empirical model, $\beta(u) = 1 - 0.70\text{erf}(u/4.5)$. In the inset, the granular drag decreases with v_s ($n = 3$). (b) Dependence of the drag reduction ratio F_r/F on $U = \omega l \tan\theta / v$. The dashed line indicates the model prediction of F_r/F. Inset shows a plot for the range of $0 < U < 8$.

We now seek a correlation for $\beta(u)$, the relative drag force for the intruder with slip to that without slip ($u = 0$). We note that granular medium around a moving object exhibits the visco-elastic characteristic, a reminiscent of a Bingham fluid.[21] The velocity profiles of shearing grains in various Couette flow systems have been successfully modeled using exponentially decaying functions.[29–31] Since the collapse of the force chains is strongly affected by the local slip velocity, we give $\beta(u)$ in the form of the error function, $\beta(u) = 1 - 0.7\text{erf}(u/4.5)$, which shows good agreement with our measurements (Fig. 4(a)). This correlation enables us to estimate the local granular drag for a rotating intruder as $dF_r \sim 2\pi\rho g(l - z)z \tan^2\theta\beta(u)dz$. The relative slip velocity is given by $u = r\omega/v = (l - z)\tan\theta\omega/v$, where r is the radius of the immersed conical intruder at the depth z below the free surface, and ω is the angular velocity. Numerically integrating dF_r with respect to z from 0 to l yields granular drag F_r for a rotating intruder at a specific angular speed.

We define the rotational drag ratio F_r/F as the ratio of the drag for a rotating intruder to that with non-rotating intruder ($\omega = 0$). Fig. 4(b) shows the dependence of the ratio on $U = \omega l \tan\theta/v$, where $\omega l \tan\theta$ corresponds to the maximum slip velocity on the contact line between the intruder and grains at the free surface. For various intruders, the reduction ratio rapidly decreases for low U but saturates as U increases further, which is in agreement with our model prediction. As the relative slip velocity increases, the measured ratio becomes slightly lower than our model because the flow experiences the transition from the quasi-static to dense flow regime where the granular medium is more easily fluidized.

In summary, we have measured the granular drag against a vertically penetrating intruder with rotation and found that the drag reduction of a rotating intruder is critically determined by the relative slip velocity. We have formulated an empirical correlation for the drag reduction by the slip motion, leading to a novel model for the drag of a rotating intruder. This model successfully describes our experimental measurements. Our work rationalizes the drag reduction of the self-burrowing seeds by rotation, which must be advantageous for the survival of the seeds before and during germination. Our study not only illuminates the functionality and beauty of natural design but also provides new insights into the design of drilling robots for military and environmental applications and underground exploration in space.[32] Visualization of the granular pressure distribution[29,33] and the granular motion[30,34] beneath the vertically penetrating rotary intruder would further our understanding of drag reduction from a microscopic point of view.

This work was supported by the National Research Foundation of Korea (Grant Nos. 2016901290, 2016913167, and 2015R1A2A2A04006181) via SNU IAMD.

[1] R. D. Maladen, Y. Ding, C. Li, and D. I. Goldman, "Undulatory swimming in sand: Subsurface locomotion of the sandfish lizard," Science **325**, 314–318 (2009).
[2] S. Jung, "Caenorhabditis elegans swimming in a saturated particulate system," Phys. Fluids **22**, 031903 (2010).
[3] A. G. Winter, R. H. L. Deits, and A. E. Hosoi, "Localized fluidization burrowing mechanics of Ensis directus," J. Exp. Biol. **215**, 2072–2080 (2012).
[4] C. Li, T. Zhang, and D. I. Goldman, "A terradynamics of legged locomotion on granular media," Science **339**, 1408–1412 (2013).
[5] A. E. Hosoi and D. I. Goldman, "Beneath our feet: Strategies for locomotion in granular media," Annu. Rev. Fluid Mech. **47**, 431–453 (2015).
[6] A. G. Bengough and C. E. Mullins, "Mechanical impedance to root growth: A review of experimental techniques and root growth responses," Eur. J. Soil Sci. **41**, 341–358 (1990).
[7] A. G. Bengough, C. E. Mullins, and G. Wilson, "Estimating soil frictional resistance to metal probes and its relevance to the penetration of soil by roots," Eur. J. Soil Sci. **48**, 603–612 (1997).
[8] N. E. Stamp, "Self-burial behaviour of Erodium cicutarium seeds," J. Ecol. **72**, 611–620 (1984).
[9] D. Evangelista, S. Hotton, and J. Dumais, "The mechanics of explosive dispersal and self-burial in the seeds of the filaree, Erodium cicutarium (*Geraniaceae*)," J. Exp. Biol. **214**, 521–529 (2011).
[10] W. Jung, W. Kim, and H.-Y. Kim, "Self-burial mechanics of hygroscopically responsive awns," Integr. Comp. Biol. **54**, 1034–1042 (2014).
[11] Y. Abraham, C. Tamburu, E. Klein, J. W. C. Dunlop, P. Fratzl, U. Raviv, and R. Elbaum, "Tilted cellulose arrangement as a novel mechanism for hygroscopic coiling in the stork's bill awn," J. R. Soc., Interface **9**, 640–647 (2012).
[12] Y. Abraham and R. Elbaum, "Hygroscopic movements in *Geraniaceae*: The structural variations that are responsible for coiling or bending," New Phytol. **199**, 584–594 (2013).
[13] R. Albert, M. A. Pfeifer, A.-L. Barabási, and P. Schiffer, "Slow drag in a granular medium," Phys. Rev. Lett. **82**, 205 (1999).
[14] I. Albert, P. Tegzes, B. Kahng, R. Albert, J. G. Sample, M. Pfeifer, A.-L. Barabási, T. Vicsek, and P. Schiffer, "Jamming and fluctuations in granular drag," Phys. Rev. Lett. **84**, 5122 (2000).
[15] I. Albert, J. G. Sample, A. J. Morss, S. Rajagopalan, A.-L. Barabasi, and P. Schiffer, "Granular drag on a discrete object: Shape effects on jamming," Phys. Rev. E **64**, 061303 (2001).
[16] K. A. Reddy, Y. Forterre, and O. Pouliquen, "Evidence of mechanically activated processes in slow granular flows," Phys. Rev. Lett. **106**, 108301 (2011).
[17] L. Bocquet, A. Colin, and A. Ajdari, "Kinetic theory of plastic flow in soft glassy materials," Phys. Rev. Lett. **103**, 036001 (2009).
[18] K. W. Desmond and E. R. Weeks, "Measurement of stress redistribution in flowing emulsions," Phys. Rev. Lett. **115**, 098302 (2015).
[19] A. Kabla and G. Debrégeas, "Local stress relaxation and shear banding in a dry foam under shear," Phys. Rev. Lett. **90**, 258303 (2003).
[20] Y. Bertho, F. Giorgiutti-Dauphine, and J. P. Hulin, "Dynamical Janssen effect on granular packing with moving walls," Phys. Rev. Lett. **90**, 144301 (2003).
[21] P. Schall and M. van Hecke, "Shear bands in matter with granularity," Annu. Rev. Fluid Mech. **42**, 67–88 (2010).
[22] F. Guillard, Y. Forterre, and O. Pouliquen, "Depth-independent drag force induced by stirring in granular media," Phys. Rev. Lett. **110**, 138303 (2013).
[23] R. Soller and S. A. Koehler, "Drag and lift on rotating vanes in granular beds," Phys. Rev. E **74**, 021305 (2006).
[24] T. A. Brzinski and D. J. Durian, "Characterization of the drag force in an air-moderated granular bed," Soft Matter **6**, 3038–3043 (2010).
[25] F. daCruz, S. Emam, M. Prochnow, J.-N. Roux, and F. Chevoir, "Rheophysics of dense granular materials: Discrete simulation of plane shear flows," Phys. Rev. E **72**, 021309 (2005).
[26] Y. Forterre and O. Pouliquen, "Flows of dense granular media," Annu. Rev. Fluid Mech. **40**, 1–24 (2008).
[27] GDR MiDi, "On dense granular flows," Eur. Phys. J. E **14**, 341–365 (2004).
[28] T. A. Brzinski, P. Mayor, and D. J. Durian, "Depth-dependent resistance of granular media to vertical penetration," Phys. Rev. Lett. **111**, 168002 (2013).
[29] E. I. Corwin, H. M. Jaeger, and S. R. Nagel, "Structural signature of jamming in granular media," Nature **435**, 1075–1078 (2005).
[30] D. M. Mueth, G. F. Debregeas, G. S. Karczmar, P. J. Eng, S. R. Nagel, and H. M. Jaeger, "Signatures of granular microstructure in dense shear flows," Nature **406**, 385–389 (2000).
[31] D. Fenistein, J. W. van de Meent, and M. van Hecke, "Universal and wide shear zones in granular bulk flow," Phys. Rev. Lett. **92**, 094301 (2004).
[32] C. Pandolfi and D. Izzo, "Biomimetics on seed dispersal: Survey and insights for space exploration," Bioinspiration Biomimetics **8**, 025003 (2013).
[33] D. M. Mueth, H. M. Jaeger, and S. R. Nagel, "Force distribution in a granular medium," Phys. Rev. E **57**, 3164 (1998).
[34] K. Sakaie, D. Fenistein, T. J. Carroll, M. van Hecke, and P. Umbanhowar, "MR imaging of Reynolds dilatancy in the bulk of smooth granular flows," Europhys. Lett. **84**, 38001 (2008).